Electrical Transport through Crossed Carbon Nanotube Junctions

Takeshi Nakanishi* and Tsuneya Ando†

*Department of Applied Physics and DIMES, Delft University of Technology
Lorentzweg 1, 2628 CJ Delft, The Netherlands

†Institute for Solid State Physics, University of Tokyo
5–1–5 Kashiwanoha, Kashiwa, Chiba 277-8581, Japan

The conductance between two crossed nanotubes is calculated in a tight-binding model and found to depend strongly on the crossing angle with large maxima at commensurate stacking of lattices of two nanotubes. The results are in good agreement with those calculated in the lowest Born approximation in an effective-mass scheme.

1. INTRODUCTION

Carbon nanotubes (CNs) are novel quantum wires consisting of rolled graphite sheets [1]. Their electronic states are quite different from those of free electrons on a cylinder surface and give rise to various intriguing phenomena. In fact, in two-dimensional (2D) graphite two bands having an approximately linear dispersion cross each other at K and K' points of the first Brillouin zone (the Fermi level, chosen at $\varepsilon = 0$). The purpose of this paper is to study electric transport through crossed single-wall CNs and to demonstrate the importance of wave-vector as well as energy conservation [2].

Recently, experimental studies of crossed CNs with electrical leads attached to each end of both nanotubes were performed and surprisingly high conductances of $0.1 \sim 0.2(e^2/h)$ were reported [3,4]. In the tunneling region with a conductance of about $0.03(e^2/h)$ power-law behavior as a function of bias voltage and temperature was observed [4], which can be described by a Tomonaga-Luttinger liquid model for tunneling [5,6]. A tunnel conductance between a CN and a graphite substrate was also reported, which suggests the importance of momentum conservation in the tunneling process [7]. Junctions of a metallic CN and a semiconducting CN were shown to behave as Schottky diodes [3].

2. CROSSED CARBON NANOTUBE

We consider a junction consisting of two crossed CNs, CNi ($i = 1, 2$), as schematically illustrated in Fig. 1. Both CNs are metallic with a circumference L. The x_i axis is chosen to be parallel to the chiral vector $\mathbf{L}_i$ and the y_i axis is parallel to the axis of CNi, where CN2 is lying on top of CN1. According to Landauer's formula [8], conductances G_{ij} are given by the sum of transmission probabilities between the jth and ith terminals as shown in Fig. 1. The

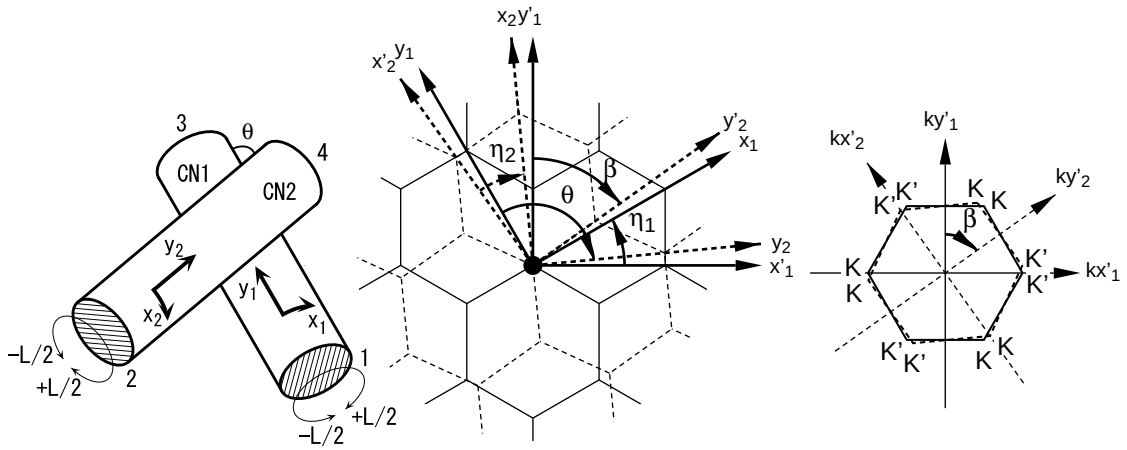

FIGURE 1. (Left) The coordinates for crossed nanotubes. θ is the angle between axes of CNs. Four terminals 1 and 3 of CN1, and 2 and 4 of CN2 are indicated.

FIGURE 2. (Middle) Lattice structure of a two-dimensional graphite sheet near the crossing of CNs. CN1 and CN2 are shown by solid and dotted lines, respectively. A view from reverse is shown for upper CN, because (x_1, y_1) and (x_2, y_2) are chosen as shown in Fig. 1.

FIGURE 3. (Right) The first Brillouin zone and K and K' points. Solid and dotted lines are corresponding to CN1 and CN2, respectively.

conductance is calculated in a single π band tight-binding model at $\varepsilon = 0$.

As a realistic model for the transfer integral between atoms in CN1 and CN2, we consider

$$t(\mathbf{R}_1, \mathbf{R}_2) = \exp\Big(-\frac{|\mathbf{d}|}{\delta}\Big)\Big[t_\sigma\Big(\frac{\mathbf{p}(\mathbf{R}_1)\cdot\mathbf{d}}{|\mathbf{d}|}\Big)\Big(\frac{\mathbf{p}(\mathbf{R}_2)\cdot\mathbf{d}}{|\mathbf{d}|}\Big) + t_\pi\big\{\big(\mathbf{p}(\mathbf{R}_1)\cdot\mathbf{e}\big)\big(\mathbf{p}(\mathbf{R}_2)\cdot\mathbf{e}\big) + \big(\mathbf{p}(\mathbf{R}_1)\cdot\mathbf{f}\big)\big(\mathbf{p}(\mathbf{R}_2)\cdot\mathbf{f}\big)\big\}\Big], \tag{2.1}$$

where $\mathbf{R}_1$ and $\mathbf{R}_2$ denote carbon sites on a 2D graphite sheet corresponding to CN1 and CN2, respectively, and $\mathbf{d} = \tilde{\mathbf{R}}_2 - \tilde{\mathbf{R}}_1$ is their distance with three-dimensional coordinates $\tilde{\mathbf{R}}_1$ of an atom on CN1 and $\tilde{\mathbf{R}}_2$ of an atom on CN2. Further, $\mathbf{p}(\mathbf{R}_1)$ and $-\mathbf{p}(\mathbf{R}_2)$ are unit vectors normal to the CN1 at $\mathbf{R}_1$ and CN2 at $\mathbf{R}_2$, respectively, and $\mathbf{d}/|\mathbf{d}|$, $\mathbf{e}$, and $\mathbf{f}$ constitute a set of three orthogonal unit vectors.

We choose the range $\delta/a = 0.325$ and the parameters $t_\sigma = 9.34\gamma_0$ and $t_\pi = -5.91\gamma_0$. They have been determined in such a way that they reproduce the structure of the π bands in bulk graphite [2]. The inter-tube distance is chosen as the inter-layer distance $D_0 = 3.35$ Å of graphite, which is larger than the distance $a/\sqrt{3} = 1.42$ Å between nearest-neighbor atoms on a graphite sheet. In this model the transfer integral decays almost exponentially with the range of about $\delta' \sim 0.8a$ as a function of the 2D distance on CN surface if the curvature is ignored.

Figure 2 shows the lattice near the crossing point. In this figure the small curvature of CNs is ignored for simplicity and η_i is the chiral angle between $\mathbf{L}_i$ and the x_i' direction fixed on each graphite plane. We introduce a parameter $\beta \equiv \theta - \eta_1 - \eta_2$ characterizing the stacking of two graphite sheets. For $\beta = \pi/3$

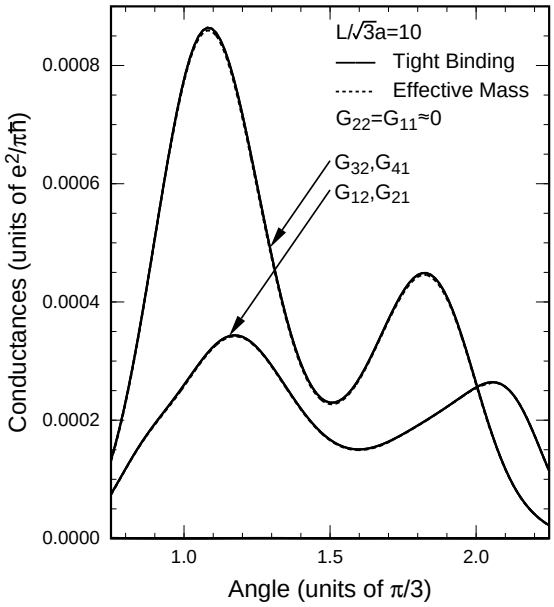

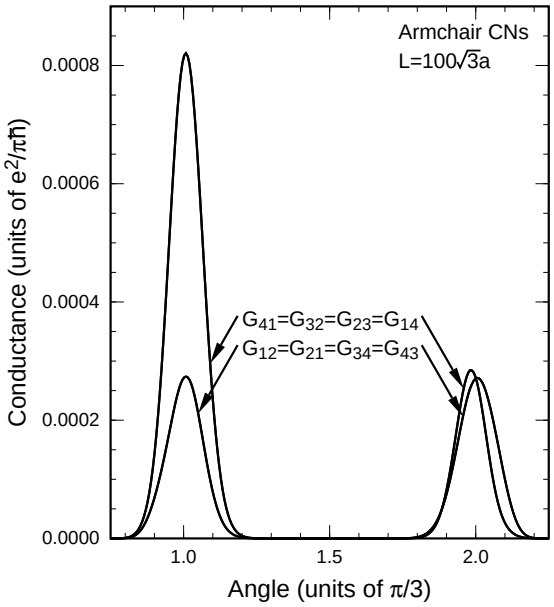

FIGURE 4. (Left) Conductances $G_{41} = G_{32}$ and $G_{21} = G_{12}$ between armchair CNs as a function of the angle θ calculated in a tight-binding model (solid lines) and in the lowest Born approximation in an effective-mass scheme (dotted lines). The reflection probabilities are vanishingly small and most of the electron wave is transmitted within each CNs, i.e., $G_{22} = G_{11} \sim 0$ and $G_{42} = G_{31} \sim 2e^2/\pi\hbar$.

FIGURE 5. (Right) Conductances $G_{41} = G_{32} = G_{23} = G_{14}$ and $G_{21} = G_{12} = G_{34} = G_{43}$ between thick CNs ($L = 100\sqrt{3}a$) calculated in an effective-mass scheme. The peak conductance is nearly independent of the circumference.

(stack I), a B site of CN2 is just above a B site of CN1 but A sites are not, just like the stacking in bulk graphite. For $\beta = 0$ (stack II), six-member rings are perfectly stacked on top of each other.

The corresponding first Brillouin zones are shown in Fig. 3. There are two Fermi points called K and K' points at the corner of the first Brillouin zone. For the stack I, the K and K' points in the (x_2', y_2') coordinate system are transformed to K and K' points, respectively, in the (x_1', y_1') coordinate system. For the stack II, the K points in the (x_2', y_2') coordinate system are transformed to K' points in the (x_1', y_1') system and vice versa. If the contact region is sufficiently large just like between graphite planes, the wave-vector conservation will determine the transmission.

3. NUMERICAL RESULTS

In explicit numerical calculations, we consider armchair nanotubes CN1 and CN2 ($\eta_1 = \eta_2 = \pi/6$), fix a B site of each CN to lie on top of each other, and rotate CNs around the B site. Figure 4 shows conductances for thin CNs with $L/\sqrt{3}a = 10$. The conductance has a broad peak at a position slightly away from $\theta = \pi/3$ and $2\pi/3$. The broadened peaks overlap and the conductance remains nonzero for all angles. The results calculated in the lowest Born approximation in an effective-mass scheme [2] are also shown in Fig. 4 by dotted lines. Both results are in excellent agreement with each other.

Numerical calculations in the realistic model become difficult for thicker nanotubes. Therefore, thicker nanotubes have been considered in a simpler model in which a transfer t_0 is possible only for atoms just on top of each other lying in a circular contact region ignoring a small curvature of CNs as in ref. [2]. The results show that tight-binding results always agree independent of the circumference with those obtained in the lowest Born approximation in the effective-mass scheme as long as $|t_0|/\gamma_0 \ll 1$. Because the inter-tube transfer integral between nearest-neighbor atoms in the realistic model is $t_0/\gamma_0 \sim -0.14$ and small, the same is expected to be applicable for the realistic model.

Figure 5 shows the conductance for thick nanotubes ($L/\sqrt{3}a = 100$) calculated in the effective-mass scheme. The conductance between two nanotubes exhibits a sharp peak at an angle corresponding to the stacks I and II but vanishingly small in other cases. This shows the importance of wave-vector conservation at crossings, which allows tunneling only between states in specific directions. Although not shown explicitly, the two peaks are broadened and their positions are slightly shifted with the decrease in the diameter. The broadening and shifts become appreciable for a thin CN as shown in Fig. 4. The broadening is due to the weakening of wave-vector conservation arising from a smaller contact area and the shift of the peak position is due to a change in the optimum condition of the interlayer transfer integrals caused by curvature effects.

4. SUMMARY AND CONCLUSION

The conductance between two crossed carbon nanotubes has been calculated in a tight-binding model and found to depend strongly on the crossing angle with large maxima at commensurate stacking of lattices of two nanotubes. The results are in good agreement with those obtained in the lowest Born approximation in an effective-mass scheme.

ACKNOWLEDGMENTS

The authors wish to thank G. E. W. Bauer and Yu. N. Nazarov for helpful discussions. This work was supported in part by Grants-in-Aid for Scientific Research and for Priority Area, Fullerene Network, from Ministry of Education, Science and Culture and by NEDO. One of us (T.N.) acknowledges the support of JSPS Postdoctoral Fellowships for Research Abroad.

REFERENCES

1. Iijima, S., *Nature (London)* **354**, 56 (1991).
2. Nakanishi, T., and Ando, T., *J. Phys. Soc. Jpn.* (submitted for publication).
3. Fuhrer, M. S., Nygard, J., Shih, L., Forero, M., Yoon, Y.-G., Mazzoni, M. S. C., Choi, H. J., Ihm, J., Louie, S. G., Zettl, A., and McEuen P. L., *Science* **288**, 494 (2000).
4. Postma, H. W. Ch., de Jonge, M., Yao, Z., and Dekker, C., *Phys. Rev. B* **62**, R10653 (2000).
5. Kane, C., Balents, L., and Fisher, M. P. A., *Phys. Rev. Lett.* **79**, 5086 (1997).
6. Egger, R., and Gogolin, A. O., *Phys. Rev. Lett.* **79**, 5082 (1997).
7. Paulson, S., Helser, A., Nardelli, M. B., Taylor II, R. M., Falvo, M., Superfine, R., and Washburn, S., *Science* **290**, 1742 (2000).
8. Landauer, R., *IBM J. Res. Dev.* **1**, 223 (1957); *Philos. Mag.* **21**, 863 (1970).